

A wireframe illustration of a car's front half, showing the engine, transmission, and front wheel. Blue lines represent airflow or fluid dynamics around the car's body. The background is a gradient of blue and white.

Proceedings

Michael Bargende  
Hans-Christian Reuss  
Andreas Wagner *Hrsg.*

# 22. Internationales Stuttgarter Symposium

Automobil- und Motorentechnik

*Band 1*

**FKFS**  
RESEARCH IN MOTION



Springer Vieweg



# Proceedings

Ein stetig steigender Fundus an Informationen ist heute notwendig, um die immer komplexer werdende Technik heutiger Kraftfahrzeuge zu verstehen. Funktionen, Arbeitsweise, Komponenten und Systeme entwickeln sich rasant. In immer schnelleren Zyklen verbreitet sich aktuelles Wissen gerade aus Konferenzen, Tagungen und Symposien in die Fachwelt. Den raschen Zugriff auf diese Informationen bietet diese Reihe Proceedings, die sich zur Aufgabe gestellt hat, das zum Verständnis topaktueller Technik rund um das Automobil erforderliche spezielle Wissen in der Systematik aus Konferenzen und Tagungen zusammen zu stellen und als Buch in Springer.com wie auch elektronisch in Springer Link und Springer Professional bereit zu stellen. Die Reihe wendet sich an Fahrzeug- und Motoren ingenieure sowie Studierende, die aktuelles Fachwissen im Zusammenhang mit Fragestellungen ihres Arbeitsfeldes suchen. Professoren und Dozenten an Universitäten und Hochschulen mit Schwerpunkt Kraftfahrzeug- und Motorentechnik finden hier die Zusammenstellung von Veranstaltungen, die sie selber nicht besuchen konnten. Gutachtern, Forschern und Entwicklungsingenieuren in der Automobil- und Zulieferindustrie sowie Dienstleistern können die Proceedings wertvolle Antworten auf topaktuelle Fragen geben.

Today, a steadily growing store of information is called for in order to understand the increasingly complex technologies used in modern automobiles. Functions, modes of operation, components and systems are rapidly evolving, while at the same time the latest expertise is disseminated directly from conferences, congresses and symposia to the professional world in ever-faster cycles. This series of proceedings offers rapid access to this information, gathering the specific knowledge needed to keep up with cutting-edge advances in automotive technologies, employing the same systematic approach used at conferences and congresses and presenting it in print (available at Springer.com) and electronic (at Springer Link and Springer Professional) formats. The series addresses the needs of automotive engineers, motor design engineers and students looking for the latest expertise in connection with key questions in their field, while professors and instructors working in the areas of automotive and motor design engineering will also find summaries of industry events they weren't able to attend. The proceedings also offer valuable answers to the topical questions that concern assessors, researchers and developmental engineers in the automotive and supplier industry, as well as service providers.

Weitere Bände in der Reihe <https://link.springer.com/bookseries/13360>

Michael Bargende · Hans-Christian Reuss  
Andreas Wagner  
(Hrsg.)

# 22. Internationales Stuttgarter Symposium

Automobil- und Motorentechnik

*Hrsg.*

Michael Bargende  
FKFS – Forschungsinstitut für Kraftfahr-  
wesen und Fahrzeugmotoren Stuttgart  
Stuttgart, Baden-Württemberg, Deutschland

IFS  
Universität Stuttgart  
Stuttgart, Deutschland

Andreas Wagner  
FKFS – Forschungsinstitut für Kraftfahr-  
wesen und Fahrzeugmotoren Stuttgart  
Stuttgart, Baden-Württemberg, Deutschland

IFS  
Universität Stuttgart  
Stuttgart, Deutschland

Hans-Christian Reuss  
FKFS – Forschungsinstitut für Kraftfahr-  
wesen und Fahrzeugmotoren Stuttgart  
Stuttgart, Baden-Württemberg, Deutschland

IFS  
Universität Stuttgart  
Stuttgart, Deutschland

ISSN 2198-7432

Proceedings

ISBN 978-3-658-37008-4

<https://doi.org/10.1007/978-3-658-37009-1>

ISSN 2198-7440 (electronic)

ISBN 978-3-658-37009-1 (eBook)

Die Deutsche Nationalbibliothek verzeichnet diese Publikation in der Deutschen Nationalbibliografie; detaillierte bibliografische Daten sind im Internet über <http://dnb.d-nb.de> abrufbar.

© Springer Fachmedien Wiesbaden GmbH, ein Teil von Springer Nature 2022, korrigierte Publikation 2022

Das Werk einschließlich aller seiner Teile ist urheberrechtlich geschützt. Jede Verwertung, die nicht ausdrücklich vom Urheberrechtsgesetz zugelassen ist, bedarf der vorherigen Zustimmung des Verlags. Das gilt insbesondere für Vervielfältigungen, Bearbeitungen, Übersetzungen, Mikroverfilmungen und die Einspeicherung und Verarbeitung in elektronischen Systemen.

Die Wiedergabe von allgemein beschreibenden Bezeichnungen, Marken, Unternehmensnamen etc. in diesem Werk bedeutet nicht, dass diese frei durch jedermann benutzt werden dürfen. Die Berechtigung zur Benutzung unterliegt, auch ohne gesonderten Hinweis hierzu, den Regeln des Markenrechts. Die Rechte des jeweiligen Zeicheninhabers sind zu beachten.

Der Verlag, die Autoren und die Herausgeber gehen davon aus, dass die Angaben und Informationen in diesem Werk zum Zeitpunkt der Veröffentlichung vollständig und korrekt sind. Weder der Verlag, noch die Autoren oder die Herausgeber übernehmen, ausdrücklich oder implizit, Gewähr für den Inhalt des Werkes, etwaige Fehler oder Äußerungen. Der Verlag bleibt im Hinblick auf geografische Zuordnungen und Gebietsbezeichnungen in veröffentlichten Karten und Institutionsadressen neutral.

Planung/Lektorat: Markus Braun

Springer Vieweg ist ein Imprint der eingetragenen Gesellschaft Springer Fachmedien Wiesbaden GmbH und ist ein Teil von Springer Nature.

Die Anschrift der Gesellschaft ist: Abraham-Lincoln-Str. 46, 65189 Wiesbaden, Germany

# Inhaltsverzeichnis – Band I

## EU7 Emission Limits

<b>Electrically Heated Catalyst for Emissions Reduction for Euro7</b> . . . . .	3
Gerd Gaiser, Tobias Lehr, and Volker Brichzin	

<b>EU 7: A First Assessment</b> . . . . .	23
Stefan Bareiss, Michael Krüger, Andreas Kufferath, Dirk Naber, Herbert Schumacher, and Marcel Wüst	

<b>Euro 7 Light Duty SCR System Solution with Software-Extraction of the Ammonia-Signal from NO<sub>x</sub>-Sensors</b> . . . . .	41
Dirk Samuelsen, David Sammet, Thomas Wahl, and Erik Weingarten	

## Electric Powertrains

<b>Optimized Drive Systems for Electric All-Wheel Drive Vehicles</b> . . . . .	59
Tobias Stoll, Michael Bargende, and Hans-Jürgen Berner	

<b>Model-Based Design and Evaluation of Future Fail-Operational Electric Drivetrains</b> . . . . .	71
Christian Ebner, Kirill Gorelik, Marcel Maier, Rainer Walter, and Christian Thulfaut	

<b>48V-CityRoadster – Safety Extra Low Voltage Traction in the Stuttgart Metropolitan Area</b> . . . . .	86
Oliver Zirn and Norbert Schreier	

## Hybrid I

<b>Hybridization and Phlegmatization of the pHCCI Diesel Engine</b> . . . . .	99
Jan Klingenstein, Andreas Schneider, Hans-Jürgen Berner, and Michael Bargende	



<b>Development of a Prediction Module for a Hybrid Operating Strategy Using Geo-Data</b> .....	114
Christian Riegelbeck, Alexander Stalp, Daniel Schade, and Christian Beidl	
<b>Innovative, modular serial hybrid concept for a highly efficient, clean automotive powertrain</b> .....	124
Christian Trapp and Maximilian Böhme	
<b>Vehicle Simulation I</b>	
<b>Highly immersive driving simulator for scenario based testing of automated driving functions</b> .....	145
Günther Prokop, Thomas Tüsch, Norman Eisenköck, and Jürgen Bönninger	
<b>Parameter Identification Using the Model Fitting Method</b> .....	155
Alfons Wagner, Hans-Christian Reuss, and Lukas Brandl	
<b>Simulation of Telecommunication and Automotive Behavior in real time</b> .....	165
Karl Schreiner, Michael Keckeisen, Tobias Rößler, and Arthur Witt	
<b>Vehicle Simulation II</b>	
<b>Measurement Data Acquisition for Off-Board Supported Diagnostic Functions – Arithmetic and Simulative View</b> .....	181
Andreas Heinz and Hans Christian Reuss	
<b>Vehicle Dynamics I</b>	
<b>Investigation of the Influence of Vehicle Payload on Rollover Behavior</b> .....	201
Christoph Ludwig, Fan Chang, Matthias Frost, Christian Schimmel, and Günther Prokop	
<b>Chassis Concept for Large Load Ranges with Integrated Level Control for the U-Shift Project</b> .....	220
Fabian Weitz, Michael Frey, and Frank Gauterin	
<b>The Future of Vehicle Development Using Virtual Prototypes and an Interconnected Software Infrastructure</b> .....	229
Alexander Ahlert	
<b>Hydrogen Powered Powertrains</b>	
<b>Automated Design of Fuel Cell Electric Vehicle Drive Systems</b> .....	247
Adrian Braumandl and Katharina Bause	

<b>Hydrogen Powertrains: A Comparison Between Different Solutions for an Urban Bus. . . . .</b>	<b>259</b>
Federico Millo, Luciano Rolando, Andrea Piano, Benedetta Peiretti Paradisi, and Afanasie Vinogradov	
<b>Modular fuel cell system test bench for the regional supplier industry. . .</b>	<b>272</b>
André Bürger, Frank Allmendinger, David Degler, Markus Jenne, Mark Bittmann, Sven Roos, Joachim Scherer, and Thomas Kiupel	
<b>Energy Efficiency in Drivetrain Development in a Mini-Grid with green H<sub>2</sub>. . . . .</b>	<b>282</b>
Bernhard Kehrwald, P. Berlet, and F. Frischholz	
<b>Combustion Engines: New Approaches</b>	
<b>High Efficiency Net Zero CO<sub>2</sub> Hybrid Powertrain . . . . .</b>	<b>295</b>
Thomas Arnold, Jan Böhme, Christoph Danzer, and Matthias Krause	
<b>Software Engineering</b>	
<b>Automotive Systems Engineering: Experiences and Guidance . . . . .</b>	<b>311</b>
Christof Ebert and Frank Kirschke-Biller	
<b>Enhancing Ground Truth for Digital Twins by Complete and Real-Time Upload of Vehicle Signals. . . . .</b>	<b>322</b>
Lorenz Görne, Hans-Christian Reuss, and Ralf Sauerwald	
<b>KI - Deep Learning I</b>	
<b>AI-based Parameter Optimization Method: Applied for Vehicles with Dual Clutch Transmissions . . . . .</b>	<b>337</b>
Marius Schmiedt, Andreas Pawlenka, and Stephan Rinderknecht	
<b>Validation Environment for Deep Reinforcement Learning Based Gear Shift Controllers. . . . .</b>	<b>354</b>
Stefan Altenburg, Katharina Bause, and Albert Albers	
<b>Data-Driven Automotive Development: Federated Reinforcement Learning for Calibration and Control . . . . .</b>	<b>369</b>
Thomas Rudolf, Tobias Schürmann, Matteo Skull, Stefan Schwab, and Sören Hohmann	
<b>Make or Buy Strategy for AI in Automotive: How Much “Make-AI” is Necessary to Succeed?. . . . .</b>	<b>385</b>
Ulrich Bodenhausen	

## **KI - Deep Learning II**

<b>Cloud-Based Predictive Diagnosis Using Machine Learning for Automotive EPGS</b> . . . . .	399
--	-----

Alia Salah, Omar Abu Mohareb, and Hans-Christian Reuss

<b>Reducing Fuel Consumption by Virtually Testing an Engine with AI</b> . . . .	414
---	-----

Joël Henry and Tilmann Oestreich

<b>Development and Testing Autonomous Vehicles at Scale</b> . . . . .	420
---	-----

Frank Kraemer

## **Combustion Engines: Modeling**

<b>Virtual Development of a New 3-Cylinder Natural Gas Engine with Active Pre-chamber</b> . . . . .	429
---	-----

Antonino Vacca, Marco Chiodi, Michael Bargende, André Casal Kulzer, Sebastian Bucherer, Paul Rothe, Ivica Kraljevic, Hans-Peter Kollmeier, Albert Breuer, and Helmut Ruhland

<b>CFD Investigation of a Burner-base Heating Strategy to Speed up the cold Start Transient of ICEs</b> . . . . .	460
---	-----

Gianluca Montenegro, Augusto Della Torre, Loris Barillari, and Angelo Onorati

## **E/E Architecture**

<b>Park Systems Evolution Out of Vehicle Architecture Evolution</b> . . . . .	477
---	-----

Nicolas Jecker

<b>Certificate-based Safety Concept for Future Dynamic Automotive Electric/Electronic Architectures</b> . . . . .	487
---	-----

Felix Krauter, Marc Schindewolf, and Eric Sax

<b>Zonal Network Architecture and CAN Networks</b> . . . . .	501
--	-----

Holger Zeltwanger

## **Charging**

<b>Wireless Charging as Key Technology for Comfortable Charging from End Customer Perspective</b> . . . . .	511
---	-----

Dennis Mehlig, Volker Schall, and Christopher Lämmle

<b>Efficient Charging of Electric Vehicles by intelligent Load Management</b> . . . . .	527
---	-----

Ursel Willrett

## Battery II

<b>Battery Development and Testing including Simulation and Function Development at ElringKlinger</b> .....	541
---	-----

Lars Weller, Pierre Freundt, Moritz Pausch, and Joachim Buck

<b>48 V Coupling of Traction and PV-Storage Battery</b> .....	555
---	-----

Oliver Zirn

## Battery I

<b>Automated Optimization of a Cell Assembly Using Format-Flexibly Produced Pouch Cells</b> .....	569
---	-----

Philip Müller-Welt, Konstantin Nowoseltschenko, Charlène Garot, Katharina Bause, and Albert Albers

<b>Field Data Analysis of a Commercial Vehicle Fleet in Relation to the Load of the HV Battery</b> .....	582
--	-----

Kerstin Hadler, Jens Michalski, Christoph Schuler, Jörg Kleemann, and Bernard Bäker

## Reports from FVV Projects

<b>Exhaust Gas Pulsation and Turbocharger Interaction</b> .....	599
---	-----

Dario Di-Modica, Philipp Nachtigal, Peter Eilts, and Jörg Seume

<b>An Empirical Based Model to Predict Ignition Delays in Partially Premixed Compression Ignition Mode</b> .....	615
--	-----

Marvin Wahl, Simon Schneider, and Michael Bargende

<b>Ash Behaviour in Wall-Flow Filters</b> .....	629
---	-----

Lukas Schneider, Matthias Kaul, Kamil Braschke, Peter Eilts, Eberhard Schmidt, and Uwe Janoske

<b>Correction to: Battery Development and Testing including Simulation and Function Development at ElringKlinger</b> .....	C1
--	----

Lars Weller, Pierre Freundt, Moritz Pausch, and Joachim Buck

<b>Autorenverzeichnis</b> .....	647
---------------------------------	-----

# Inhaltsverzeichnis – Band II

## VEHICLE TECHNOLOGY

<b>Individualization of the drive types with the overall vehicle concept for small commercial vehicles</b> .....	3
Jürgen Erhardt	

<b>Blockchain-based Test Management in Full Vehicle Testing</b> .....	11
Oliver Braun and Johannes Eckstein	

<b>U-Shift II Vision and Project Goals</b> .....	18
Marco Münster, Mascha Brost, Tjark Siefkes, Gerhard Kopp, Elmar Beeh, Frank Rinderknecht, Stephan Schmid, Manuel Osebek, Sebastian Scheibe, Robert Hahn, David Heyner, Philipp Klein, Giovanni Piazza, Christian Ulrich, Werner Kraft, Franz Philipps, Lennart Köhler, Michael Buchholz, Thomas Wodtke, Klaus Dietmayer, Michael Frey, Fabian Weitz, Frank Gauterin, Hannes Stoll, Marc Schindewolf, Houssem Guissouma, Felix Krauter, Eric Sax, Jens Neubeck, Sven Müller, Sven Eberts, Michael Göldner, Stephan Teichmann, Jochen Kiebler, Miralem Saljanin, Michael Bargende, and Andreas Wagner	

## E-MOBILITY

<b>The Development of a Heat Pump Based EV Thermal Management System</b> .....	35
Y. Guo, C. Wei, Y. Wang, H. Sheng, J. Wu, and Z. Guo	

<b>Well-to-Wheel Evaluation of Conventional and Alternative Powertrains for Municipal Refuse Collection Vehicles</b> .....	45
Nicolas Hummel, Patrick Noone, Christian Beidl, and Niklas Kirschner	



**HYBRID II**

**Intelligent Data Analytics with Artificial Intelligence for Hybrid Engine Restart . . . . .** 61  
Florian Schuchter, Katharina Bause, and Albert Albers

**AUTOMATION I**

**Novel Approach for Vehicle-Self-Localization . . . . .** 75  
Jochen Kiebler, Miralem Saljanin, Sven Müller, Smiljana Todorovic,  
Jens Neubeck, and Andreas Wagner

**Virtual Validation of Automated, Autonomous and Connected Mobility at the University Campus of Stuttgart . . . . .** 89  
Ralf Frotscher, Frank Beutenmüller, Andreas Kirstädter, Dan Keilhoff,  
and Hans-Christian Reuss

**AUTOMATION II**

**Situation Awareness Management for Driver Take Over from Level 4 . . .** 101  
Christian Pfeifer, Philipp Pomiersky, and Wolfram Remlinger

**User-Oriented Development of Autonomous Vehicles using Immersive Visualization Tools . . . . .** 112  
Lars Everding, Christian Raulf, Melanie Klapprott, and Thomas Vietor

**ELECTRIC MOTORS**

**Contribution of Fully Non-Magnetic Metal Materials to The Efficiency Enhancement of Electric Engines . . . . .** 127  
Stefan Lindner

**Calculation and Experimental Characterization of the Stiffness of Laminated Back Iron for Rotors of Axial Flux Machines . . . . .** 137  
M. Fuchslocher, T. Albrecht, S. Henzler, M. Bargende, and M. Raible

**Synergetic 1D–3D Reduced Order Modeling Techniques for Electric Motor Design Analysis . . . . .** 152  
Dig Vijay and Nils Framke

**DRIVING RESISTANCE**

**Investigations into the Aerodynamic Influence of Trailers Towed by Battery Electric Passenger Cars . . . . .** 171  
Etienne Pudell and Christopher Edelmann

**Sensatorq, a New Approach for Measure the Forces at Wheels and Apply these to Vehicle Dynamics Control of the Future Mobility . . .** 183  
Christian Schotte

<b>On the Importance of Highly Resolved Wind Forecasts for Range Estimation . . . . .</b>	<b>187</b>
Rafael Abel, Lutz Pegel, and Andreas Waldmann	

## **TEST & VALIDATION II**

<b>Breaktor™ Battery Disconnect Unit: Advanced Protection and Power Distribution for High Voltage Circuits in Electric Vehicles . . . . .</b>	<b>199</b>
Mike Lau and Kevin Calzada	

<b>A Modular Co-Simulation Framework with Open Source Software and Automotive Standards . . . . .</b>	<b>207</b>
Dominik Salles, Lukas Lang, Martin Kehrer, and Hans-Christian Reuss	

<b>The Use of Modern IT Architectures in Complex Test Scenarios of Systems Engineering . . . . .</b>	<b>224</b>
Björn Hansen and Thomas Rönpage	

## **TEST & VALIDATION I**

<b>Method for the Automatic Generation of Vehicle-Specific Individual Test Sequences . . . . .</b>	<b>231</b>
Hans Christian Reuss	

<b>Virtual World Meets Reality – Validation of Advanced Driver Assistance Systems . . . . .</b>	<b>246</b>
Rolf Magnus and Björn Butting	

## **EMISSIONS I**

<b>Empirical Temperature Modelling of the Diesel Oxidation Catalyst. . . . .</b>	<b>263</b>
Andreas Schneider, Jan Klingenstein, Hans-Jürgen Berner, and Michael Bargende	

<b>Remote Sensing Measurements and Simulations for Real Driving Emission Characterization of Vehicles . . . . .</b>	<b>277</b>
Justin Plogmann, Ariane Gubser, and Panayotis Dimopoulos Eggenschwiler	

<b>Simulation of Particle-Agglomerate Transport in a Particle Filter using Lattice Boltzmann Methods . . . . .</b>	<b>292</b>
Nicolas Hafen, Mathias J. Krause, and Achim Dittler	

## **EMISSIONS II**

<b>Modeling of NO and CO Raw Emissions Based on Mixture Inhomogeneities in SI Engines . . . . .</b>	<b>307</b>
Daniel Ismail Mir, Michael Grill, Michael Bargende, Fabian Steeger, Marco Günther, and Stefan Pischinger	

**A Model Approach to Simulate Exhaust Gas Temperatures of Diesel Oxidation Catalysts. . . . . 323**  
Tobias Stoll, Jan Klingenstein, Andreas Schneider, Michael Bargende, and Hans-Jürgen Berner

**COMPONENTS I**

**Auditory perceived quality of manual-mechanical control elements in cars. . . . . 337**  
Michael Tondera, Florian Reichelt, Lutz Fischer, Franziska Kern, Jonathan Kiessling, Daniel Holder, and Thomas Maier

**Answering Challenges in Oil Filter Systems for e-Axles and modern high efficient Transmissions. . . . . 350**  
Claudia Wagner, Richard Bernewitz, Marius Panzer, Anna-Lena Winkler, and Alexander Wöll

**Automatic Bearing Damage Detection on Commercial Vehicle Cardan Shafts . . . . . 359**  
Chris Auer and Hans-Christian Reuss

**COMPONENTS II**

**Towards an Emission-Neutral Vehicle by Integrating a Particulate Filter System into the Frontend. . . . . 371**  
E. Thébault, V. Raimbault, B. Junginger, M. Dos Santos Ascensao, Q. Montaigne, D. Chalet, G. Opperbeck, and F. Keller

**Novel, More Climate-Friendly, Multifunctional Light Metal Parts for Multidisciplinary Applications. . . . . 387**  
Eugen Pfeifer

**Volume Forecasts of Passenger Car Sales and Correspondding Metallic Components of VW Group Until 2030. . . . . 400**  
Mathias Liewald and Nicolas Rose

**VEHICLE DYNAMICS II**

**Method for the Determination of Objective Evaluation Criteria Using the Example of Combined Dynamics. . . . . 427**  
Justus Raabe, Fabian Fontana, Jens Neubeck, and Andreas Wagner

**A Validated Set of Objective Steering Feel Parameters Focusing on Non-Redundancy and Robustness . . . . . 443**  
Erik Ketzmerick, Patrick Zösch, Hendrik Abel, Thomas Enning, Christian Schimme, and Günther Prokop

**Autorenverzeichnis . . . . . 467**

## **EU7 Emission Limits**



# Electrically Heated Catalyst for Emissions Reduction for Euro7

Gerd Gaiser<sup>(✉)</sup>, Tobias Lehr, and Volker Brichzin

Purem GmbH, Esslingen, Germany

{gerd.gaiser,tobias.lehr,volker.brichzin}@purem.com

**Abstract.** For Euro7 real driving cycles require an increase in exhaust gas temperature at cold start. This paper presents results on the emissions reduction effects of using an electric heating catalyst. Different heating strategies for diesel and gasoline engines are discussed. The application in diesel engines requires a high heat input into the exhaust gas already at very low mass flows in order to heat up also the downstream components of the SCR system quickly. Measurements and simulations are used to show how the heat input is influenced by the geometry and the heat transfer surface of the heating element and how this is affected under different operating conditions. Measurements on the engine test bench show the potential for emission reduction. In addition, it is shown that a catalytic coating of the heating element results in a further increased emission reduction. Particular emphasis is placed on robustness in operation. The presented Lamella Heater is tolerant to fuel and AdBlue and due to its fully insulated design insensitive to condensate and particles.

**Keywords:** Catalyst heating · Coldstart · Emission Reduction

## 1 Introduction

All scenarios for the introduction of Euro7 envisage a reduction in emission limits, while at the same time additional limits are set for other exhaust components. The most stringent measure is the required compliance under RDE driving conditions, which may also include exceptional worst-case driving.

Challenges arise in cold start and low-load operation. For example, a cold start with an immediately following acceleration phase before the catalytic converter is heated sufficiently is particularly challenging, especially since engine heating measures have their limits during this time as long as the catalytic converter is not yet fully at its operating temperature. In these cases, an electric heating element can quickly heat-up and maintain the catalytic converter at its operating temperature. In this way, emissions can be significantly reduced. Electrical heating of catalysts was already known in earlier times [1] and is also currently being considered in many cases [2]. Different concepts are also studied in the literature [3, 4].



Different applications lead to diverging requirements for the heating element. An effective design must therefore be based on the respective application.

## 2 Requirements for a Heating Element for Different Applications

**General requirements.** A basic requirement is the rapid heating of the heating element. For the required performance and power demand, operation at 48 V is usually mandated. This usually requires a separate 48 V ground connection separate from the vehicle ground. The power should be continuously adjustable. In addition to a robust design, the heating element should also be insensitive to condensate, water droplets and soot particles. For the pre-SCR arrangement discussed later on, the heating element should also be insensitive to exposure to AdBlue droplets and their decomposition products. The optional catalytic coating capability shown later is also an important criterion.

**Application for Diesel engines.** The lower exhaust gas temperatures of diesel engines makes longer heating operation necessary in the driving cycle. After the immediate cold start, further auxiliary heating with medium modulated heating power is required here in low-load phases too. Besides the required fast DOC heat up, Diesel engines in addition require a very fast heat up of the subsequent SCR catalyst to its operating temperature. As the heat transfer to these downstream components takes place via the exhaust gas, thus the requirement for high heat transfer from the heater to the exhaust gas is derived from this. This requires a large heat transfer surface and a high heat transfer coefficient.

**Application for Otto engines.** In normal operation, the exhaust gas temperatures of Otto engines are higher, so that auxiliary heating is only necessary during a short cold-start phase. Depending on the operating strategy, the heating measure can already be stopped after the first 30–60 s after engine start. In order to heat the TWC to its operating temperature very quickly at the beginning of this very short period, a very large heating power is required on the one hand, and a low heat capacity of the heater on the other. The aim here is to bring the catalytic surface of the 3-way catalyst (TWC) quickly up to reaction temperature. Downstream components such as the Otto particulate filter do not require any additional heat.

A catalytic coating on the heating element itself is here of particular advantage. It is brought up to the reaction temperature many times faster than the subsequent catalyst. The only limitation is the limited surface area of the heating element.

Preheating prior to engine start is often regarded as an additional heating phase during the startup process. The resulting aspects are discussed in Sect. 6.

**Application for PHEV powertrains.** When the combustion engine is switched on at the end of each electrically driven phase, a small cold start results. Then a differently pronounced auxiliary heating may be required, depending on the driving condition and duration of the electrically driven phase. Due to the vehicle electrical system architecture, there is often a desire for direct operation of the heater with 400 V on the high-voltage vehicle electrical system.

### 3 Lamella Heater

To meet these above mentioned requirements, the Lamella Heater described below is developed. The Lamella Heater is designed as a separate heating element, with an inherently stable structure independent of the downstream catalyst. The Lamella Heater can be used with both ceramic and metallic catalysts and is usually integrated into the catalyst housing.

#### 3.1 Setup

The Lamella Heater consists of a metal sheathed heating conductor with fins made of lamellas, which ensure a high heat transfer. Figure 1 shows two exemplary designs. The core of the sheathed heating conductor is designed in its resistance for the respective heating power. This core is encased in a mineral insulating layer, which insulates it electrically from the metallic sheath. The metallic jacket creates a very robust structure that electrically insulates the core heating conductor fully from the exhaust gas and exhaust system. The thermal conductivity of the electrical insulation layer ensures good heat transfer from the heating core to the metallic sheath.

The heating conductor is led out of the exhaust system in a metallically insulated manner and is electrically contacted outside the exhaust system. The core heating conductor is contacted via the two pins at the respective ends and is thus insulated from the metallic sheath and the exhaust system. The metal-insulated cold sections remain unheated but are just as temperature-stable as the heated section. The length of the cold sections outside the exhaust system can be customized. For example, the metal-insulated cold sections can be routed through a shielding plate and the contacting with the connecting cable can then be made in the colder shielded area.

To achieve the high heat transfer, the lamella fins are brazed to the sheath heating conductor with a high temperature brazing material at more than 1150 °C. The Lamella Heater is temperature resistant up to 1000 °C. Heating of the heating conductor occurs only in the finned area. The unfinned ends and the feedthrough are designed as cold parts. The finning consists of a continuous lamellar strip so that the respective fins have a rectangular surface. The resulting connection of adjacent fins allows a high stability of the fins and a fixed fin spacing to be achieved. The mechanical bearing is provided by a support structure and is connected to the housing shell.

The lamella fins can optionally be catalytically coated. In this case, direct heating of the catalytically active layer thereon can be achieved. This coating on the heater itself reaches the light-off temperature much faster than the downstream catalyst.

#### 3.2 Characteristics

Due to its electrically fully insulated design, the Lamella Heater is completely insensitive to condensate, water droplets, and soot particles. This also allows it to be used in a pre-SCR position discussed later, where it can be exposed to AdBlue spray. The fully electrically insulated design also avoids the occurrence of leakage currents.

In addition, the fully insulated design also allows an optional high-voltage version (e.g. 400 V) for direct operation on the high-voltage vehicle electrical system.

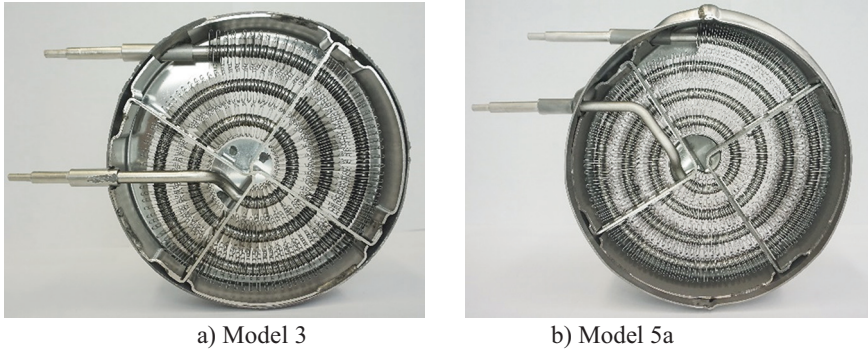


**Fig. 1.** Structure of the Lamella Heater in two exemplary versions. a) model 3 (left picture) b) model 5a (right picture)

Figure 1 shows two exemplary designs of the Lamella Heater used in the tests described below. Model 3 shows a round design for direct insertion into the catalyst housing. Model 5a shows a design with a larger surface area and larger free cross-section for welding into the catalyst housing. Table 1 shows some characteristics of the two setups. Model 3 is designed for a maximum heat output of 4.5 kW or optionally 6 kW. Model 5a is designed for a maximum heating capacity of 6.5 kW, each at 48 V. The heat transfer surface in model 5a was increased to 0.29 m<sup>2</sup> by changing the fin geometry and number of fins. In another model 5c, not shown here, the heat transfer surface was further increased to 0.32 m<sup>2</sup>. It will be shown later that the larger heat-transferring surface area of model 5a and 5c further increases the heat output that can be transferred to the exhaust gas at low mass flows.

**Table 1.** Characteristics of the two example setups used in the experiments shown later on.

	Model 3	Model 5a
Heating power	4.5 kW or 6 kW @ 48 V	6.5 kW @ 48 V
Length	32 mm	26 mm
Open frontal area	78%	94%
Geometric surface of lamella fins	0.21 m <sup>2</sup>	0.29 m <sup>2</sup>
Optional catalytically coatable	Yes, optional	Yes, optional

## 4 Heat Transfer and Heating Power

### 4.1 Simulation Model for Heat Transfer

A 1D simulation model was developed in Matlab for the design of the Lamella Heater. The model allows the simulation of the internal heating behavior of the heating element, the heat transport inside the heating conductor, the heat conduction into the fins and the heat transfer to the exhaust gas. This makes it possible to simulate and optimize both the internal structure of the heating element and the geometric design of the fins in terms of their effect on the heating of the exhaust gas and the surface. The calculation of heat conduction and heat transfer at the fins is based on [5]. The calculation of heat transfer coefficients is based on [6]. The structure of the model is described elsewhere due to space constraints [7].

Figure 2 shows an example of calculated temperatures of the heating element, fin surface and exhaust gas in comparison with values measured in the experiment. In this example, a WLTC cycle was simulated for a diesel engine with a heating element power input of up to 4 kW corresponding to the comparable experiment. The heating power was modulated by a controller to achieve a target exhaust gas temperature of 250 °C downstream of the heating element.

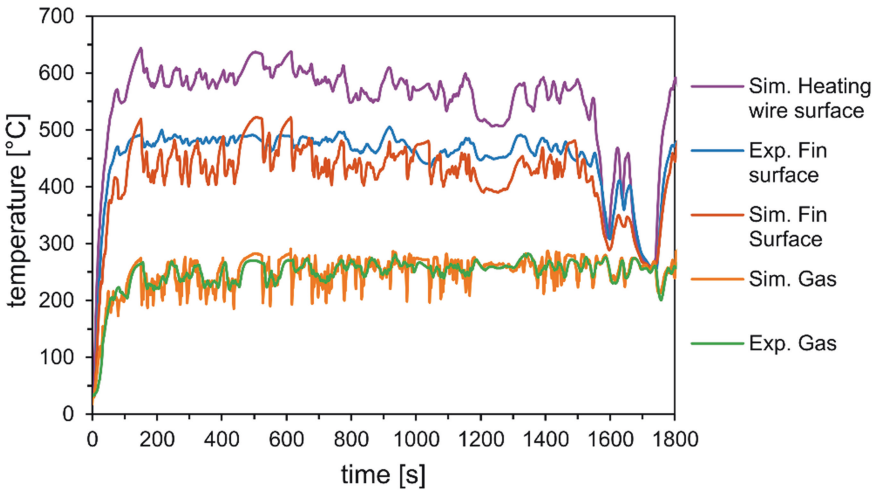


**Fig. 2.** Surface and gas temperatures at the heating element under WLTC conditions for a Diesel engine (Simulations and Experiments).

The upper line shows the temperature at the surface of the sheath heating conductor. The two middle lines show the temperature of the fin surface. The fin temperatures show a somewhat smoother curve in the measured values; this follows from the thermal inertia of the thermocouple used in the experiment. Furthermore, the measured temperatures are somewhat higher. The reason for this is that the thermocouple is located closer to the base of the fin, while the simulated curve shows

the average fin temperature. The two lower lines show the gas temperature behind the Lamella Heater. Remarkable is the very good agreement between simulated and measured gas temperature, the lines are practically on top of each other. Due to the thermal inertia of the thermocouple used in the experiment the measured temperatures do not exactly follow the high dynamic as the simulated ones do.

The values show that in this drive cycle the required heat conductor sheath temperatures are in the range around 600 °C. This is far from the maximum permissible temperature of 1000 °C; which provides a large thermal robustness against overtemperatures and allows here a simpler control without continuous thermal monitoring of the heating element.

## 4.2 Heating Power – Operating Map

For heating the exhaust gas during cold startup, it is crucial that a highest possible heating power can be introduced into the exhaust gas even at the low mass fluxes in the cold start phase. This requires a large heat transfer surface and high heat transfer coefficients. Figure 3 shows the heat output that can be permanently introduced into the exhaust gas under steady-state conditions as a function of the exhaust gas mass flow for the two versions of the Lamella Heater shown in Fig. 1. Model 3 is available as a 4.5 kW or optionally as a 6 kW version. In this version, the heating capacity of 6 kW can be permanently introduced from an exhaust gas mass flow of 70 kg/h and above.

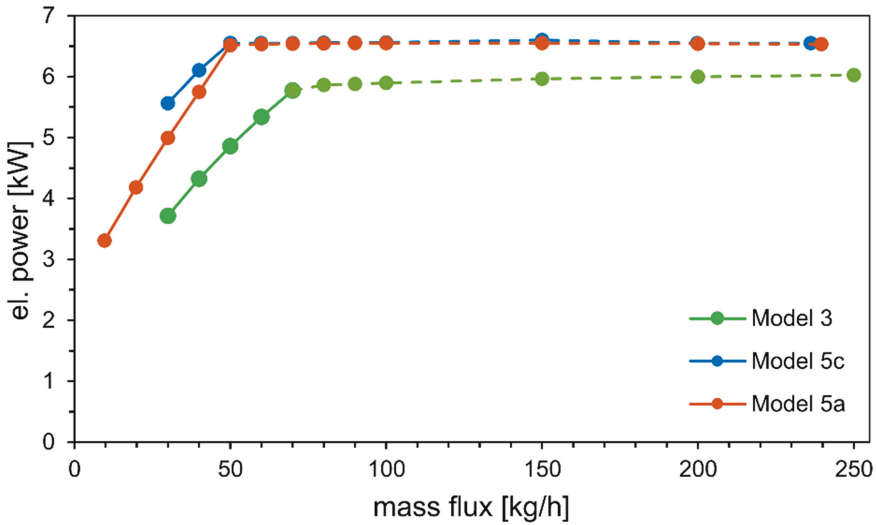


Fig. 3. Heating power depending on the exhaust mass flux (for steady conditions)

The Model 5a version of the Lamella Heater has a significantly larger heat-transferring surface and, due to the further optimized fin design, also a higher heat transfer. Therefore, with this design, a heating capacity of 6.5 kW can be permanently



introduced into the exhaust gas even at small exhaust gas mass flows of 50 kg/h. Even at a very low mass flow of 30 kg/h, a power of 5 kW can be permanently applied without overheating the heater. Another model 5c design with a yet further improved heat transfer surface compared to model 5a achieves a yet higher power at very low mass fluxes.

This power limitation applies to stationary continuous operation and is mapped via a temperature-dependent characteristic diagram. During the initial heat-up phase, the heaters can each be operated at their full power, i.e. 6.5 kW in the case of model 5a.

## 5 Application Example Diesel Engines

This section describes the use of the Lamella Heater for emission reduction in the case of a diesel engine. In this example, the Model 3 described above was used in the version with the smaller nominal power of 4.5 kW.

### 5.1 Setup on the Test Bench

These tests were carried out on the engine test bench using a 2 L diesel engine. For these tests, a WLTC cycle was run on the dynamic engine test bench. A series exhaust system was used for the setup. The Lamella Heater was installed in front of the DOC. The diameter of the heater was matched to the diameter of the DOC. The DOC was moved back by the length of the heater. Temperatures were measured before and after the heater at several locations to eliminate inhomogeneities. Additional temperatures were recorded in and after the DOC, and before and after the SDPF. Further measurement points were recorded along the entire exhaust system.

The exhaust gas composition was measured with a 2-line FTIR. The first line recorded the raw emissions in the cone after the turbocharger before the heater. The second line recorded the emissions downstream of the DOC. Due to space constraints in the exhaust system, the sampling probe of the second line was inserted through the nozzle of the SCR injector. Therefore, AdBlue dosing was not possible in this test.

The heating power of the Lamella Heater is provided via a control unit. In this test, heating starts after the engine is started. The output of the Lamella Heater is controlled via the control unit. The controlled variable is the target temperature 250 °C behind the DOC. To minimize the reaction time due to the heat capacity of the DOC, the control is performed as feedforward control of the enthalpy difference between the temperature before the heater and the target temperature, considering the current mass flow. The measured temperature downstream of the DOC is fed into the subordinated balancing controller.

### 5.2 Effect on the Temperature Behavior

The tests are carried out without any engine-based heating measures in order to evaluate the potential of the heater alone. Figure 4a shows the resulting heating power in the WLTC cycle. Figure 4b shows the exhaust gas temperatures before the heater

(blue line) and the temperature after the Lamella Heater (green line). Until the target temperature is reached, the control utilizes the full 4.5 kW heater power. When the target temperature of 250 °C after DOC is reached, the temperature control applies and modulates the heating power depending on the exhaust gas mass flow and exhaust gas temperature. Since no engine-based heating measures were used in the test shown here, additional heating via the heater is necessary in almost the entire cycle. Only in the final phase at high speeds the inlet temperature is sufficiently high and the heater is switched off. Figure 4b illustrates the increase in exhaust gas temperature by the heater in the cycle.

Figure 4c shows the temperature at the surface of the heater. Due to the high heat transfer at the large fin surface, the heating power is already introduced into the exhaust gas at moderate temperatures of the heater surface in the range of 500 °C. This means that there is a high degree of safety against overtemperatures and thus there is potential for easy control. Another advantage is that the heater reaches these moderate temperatures quickly.

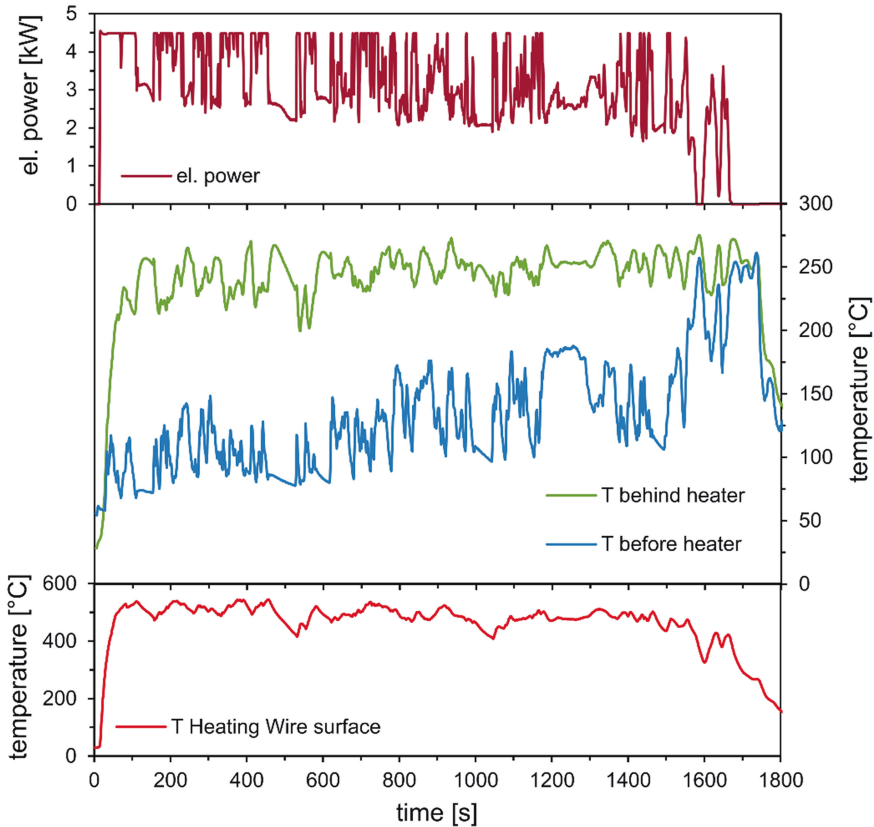


**Fig. 4.** Effects of the Lamella Heater on Exhaust Temperature in the WLTC Cycle for a 2 L Diesel engine. 4a) Applied heating power (top); 4b) Exhaust temperature rise by the Lamella heater (center); 4c) Heater surface temperature (bottom).

### 5.3 Effect on Emission Reduction

By raising the exhaust gas temperatures through the heater, emissions can be significantly reduced in the cold start and low-load range. Figure 5 shows the emission values after the DOC for NMHC. Shown are the cumulative NMHC emissions over the driving distance of the WLTC. The upper blue line shows the emissions for the case without Lamella Heater. Due to the low exhaust gas temperatures, only a moderate conversion occurs.

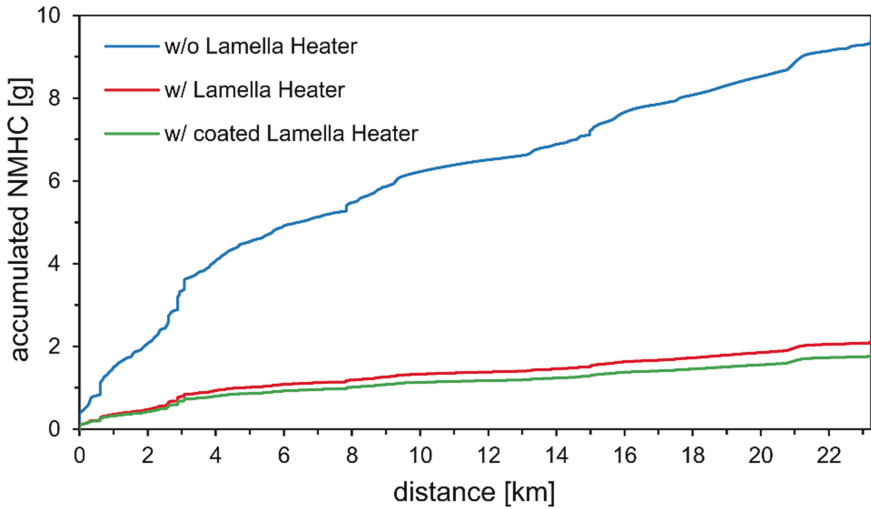


**Fig. 5.** Cumulative NMHC Emissions along the driving distance in the WLTC with and without Lamella Heater.

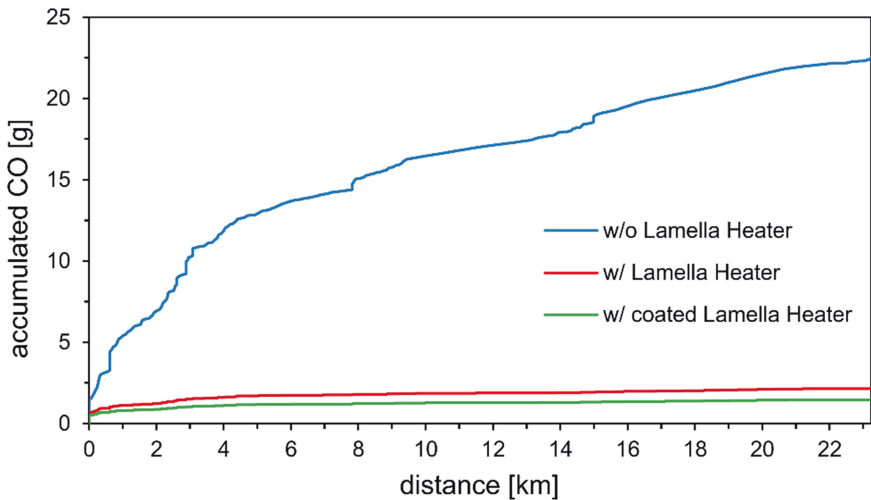


**Fig. 6.** Cumulative CO Emissions along the driving distance in the WLTC with and without Lamella Heater.

The reduced emissions due to auxiliary heating with the Lamella Heater are shown in the red line and illustrate the great potential. Supplementary exhaust gas heating with the Lamella Heater can reduce NMHC emissions by almost 80% compared to the unheated case.

The effect on CO emissions is shown in Fig. 6. The cumulative CO emissions over the driving distance of the WLTC are shown. Again, the blue curve shows the emissions after DOC for the case without a heater. The large potential due to auxiliary heating with the Lamella Heater becomes obvious. By heating with the Lamella Heater, CO emissions can be reduced by more than 90% compared to the unheated case.

The increase in exhaust gas temperatures by the Lamella Heater also offers great potential for reducing  $\text{NO}_x$  emissions of diesel engines. Figure 7 shows the exhaust gas temperatures downstream of the DOC, so immediately upstream of the AdBlue dosing point, during the WLTC cycle in the test described above. The blue line shows the temperatures without heater. The upper red line shows the temperature at this same point for the case with the Lamella Heater.

The temperature of 200 °C required for activation of the SCR system is reached much earlier with the heater. Without heating, the 200 °C at this point will only be reached after 1580 s. Heating with the Lamella Heater reduces this time to activation of the SCR system to 59 s.

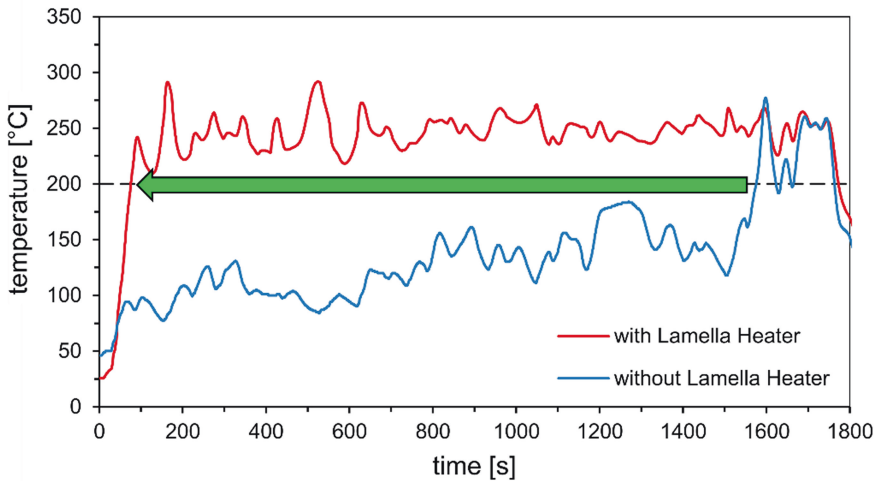


**Fig. 7.** Effects of Lamella Heater on the time needed to reach the SCR activation temperature.

Figure 8 illustrates the potential that results from this for the reduction of  $\text{NO}_x$  emissions. The blue line shows the cumulative raw  $\text{NO}_x$  emissions measured in the WLTC during this test until the temperature of 200 °C is reached. This occurs in the unheated case after the 1580 s determined from Fig. 7. Assuming that the SCR system is activated after this time and assuming a  $\text{NO}_x$  conversion of 95% with the SCR

system after its activation, the emissions will then only increase in accordance with this conversion. This is shown in the continuation of the blue line after this point in time. This results in a calculated value for the cumulative  $\text{NO}_x$  emissions at the end of the cycle.

The red line shows the comparable calculation for the case with the Lamella Heater. No  $\text{NO}_x$  conversion takes place until the temperature of 200 °C is reached. In this case, the temperature of 200 °C is reached after 59 s, as already determined from Fig. 7. Assuming the same conversion of 95% with the SCR system after its activation, the further course of the cumulative  $\text{NO}_x$  emissions is then calculated in the same way resulting in the red line. The comparison of the two values at the end of the cycle shows a potential for reducing the cumulative  $\text{NO}_x$  emissions by 91% by heating the exhaust gas with the Lamella Heater.

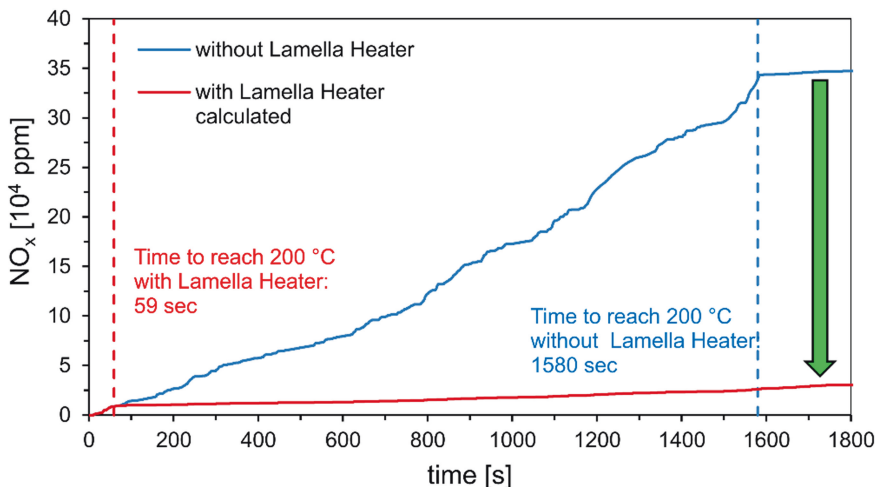


**Fig. 8.** Potential for  $\text{NO}_x$  emission reduction by earlier activation of the SCR system in case of the Lamella Heater.

#### 5.4 Effect of a Catalytic Coating on Emission Behavior in the WLTC Cycle

For further emission reduction, the Lamella Heater can optionally be catalytically coated. Figure 9 shows the test model 3 sample used here with a DOC coating. For the installation on the test rig, the test setup was provided with a flange.

The same WLTC tests were carried out with the coated test sample. The results are also included in Figs. 5 to 7 and compared to the uncoated case. The green line in Fig. 6 shows the cumulative CO emissions for the case with catalytic coating compared with the case of the uncoated heater. The comparison shows that the coating can lower the CO emissions even further. The curve of the cumulative NMHC emissions in the WLTC cycle is included in Fig. 5. Here, too, the DOC coating of the Lamella Heater results in a further reduction of the cumulative NMHC emissions.

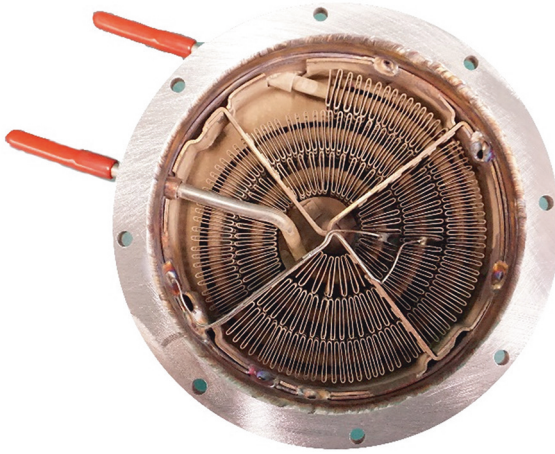


**Fig. 9.** Lamella Heater model 3 with a catalytic DOC coating.

Figure 10 shows a comparison of the emission values achieved in the different cases for CO and NMHC. The blue columns show the emission values without Lamella Heater, the red columns show the emission values with uncoated Lamella Heater and the green columns show the emission values with the DOC-coated Lamella Heater. The uncoated heater can reduce the cumulative CO emissions in the WLTC cycle by 90% compared to the unheated case. By using a catalytic coated Lamella Heater, CO emissions can be reduced by an additional 32%. The cumulative NMHC emissions in the WLTC cycle are already reduced by 78% by the uncoated heater. The DOC coating of the heater also results in a reduction of cumulative NMHC emissions by a further 16%.

The coated active surface is decisive for the catalytic effect. A larger surface area, such as in model 5a of the Lamella Heater, can therefore further increase the emission reduction by the catalytic coating. Furthermore, the DOC coating of the heater also leads to a beneficial  $\text{NO}_2/\text{NO}_x$  ratio in a shorter time.

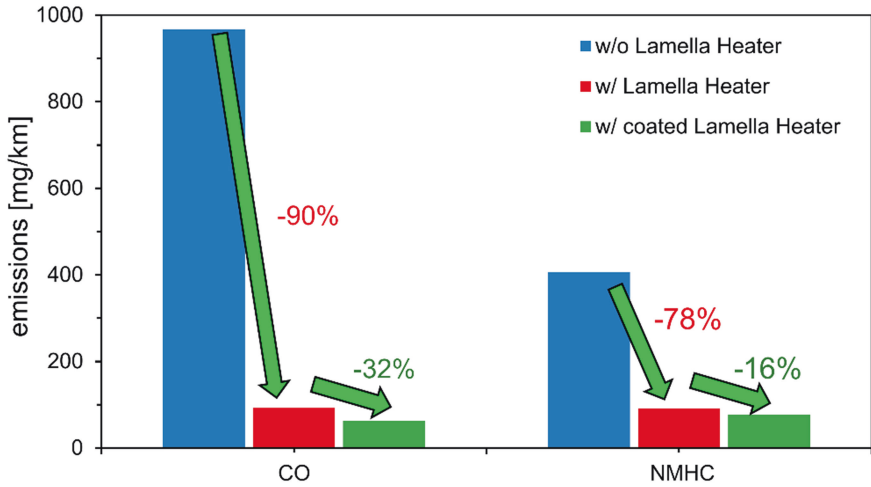


Fig. 10. Emission reduction by Lamella Heater without and with catalytic coating.

## 6 Application Example Otto Engine

In this section, the application of the Lamella Heater for emission reduction in case of Otto engines is considered. In this example, the model 5a of the Lamella Heater described at the beginning was used in the version with the nominal power of 6.5 kW. The Lamella Heater was initially uncoated in this series of tests in order to first investigate the effect of the heating-only measure on emission reduction. The effects of an optional catalytic TWC coating are then shown in Sect. 6.3.

### 6.1 Setup on the Test Bench

These tests were carried out on the engine test bench using a 1.5 L Otto engine. The effect of emission reduction in the WLTC cycle is shown in the following section. The Lamella Heater is installed directly in front of the three-way catalytic converter (TWC). The diameter of the heater is matched to the diameter of the TWC and the TWC was moved backward by the length of the heater. Temperatures were measured before and after the heater at several locations to eliminate inhomogeneities. Additional measurement points were recorded along the entire exhaust system.

A 2-line FTIR was used to measure the exhaust gas composition. The first line recorded the raw emissions in the cone before the heater. The second line recorded the emissions after the TWC.

### 6.2 Effects of Heating Strategy on Emission Reduction

The power output of the Lamella Heater is regulated via a control unit. The development of an Eberspächer control unit for modulated switching of high currents is

presented elsewhere. Experiments with different heating strategies are presented below. At first heating starts with engine start and as a secondary option a preheating is conducted before the engine start.

**Heating from engine start.** In the series of tests shown first, heating started at the same time when the engine was started. In order to heat up the catalyst as quickly as possible, heating is carried out from the engine start with a maximum heating power of 6.5 kW. The maximum heating power is applied until the temperature after the TWC exceeds a specified target temperature, e.g. 400 °C, for the first time. If a higher target temperature is selected, the heating measure can then be terminated in most applications. If a challenging driving cycle requires it, the heater can optionally also be operated further to ensure that the target temperature is maintained even under conditions such as a long downhill phase.

The effect of the Lamella Heater on the NMHC emissions in the WLTC cycle is shown in Fig. 11. The diagram shows the cumulative NMHC emissions after the TWC. The blue line shows the case without Lamella Heater. The curve shows the dominating influence of the cold start emissions especially on the first kilometers of the driving distance. After that, the cumulative emissions only increase slowly. The engine used here exhibits comparatively low exhaust gas temperatures. In conjunction with the catalyst size used, this results in a further slow increase in cumulative emissions after the cold start. This could be reduced by an adapted engine calibration.

The red line shows the case when heating with the Lamella Heater from engine start. The Lamella Heater is operated here for 60 s with a heating power of 6 kW. Afterwards the Lamella Heater was heated for 90 s with a reduced output of 3 kW. As a result of the heating, the reduction in emissions is already apparent immediately after the engine is started. After the first kilometer, emissions are reduced by 56%. In the further course, there is no more heating; therefore the emissions diagram runs parallel to the case without heater.

**Preheating without mass flow before engine start.** To further accelerate the heating of the catalyst, electrical preheating before engine start is often considered. This is also often considered in conjunction with a carrier airflow from a secondary air blower. This influence will be considered in the next section.

First, the preheating before the engine start without mass flow is considered in this test. Different preheating times were investigated. Preheating times of 15 and 30 s are shown below. The effect on NMHC emissions is also shown in Figs. 11 and 12.



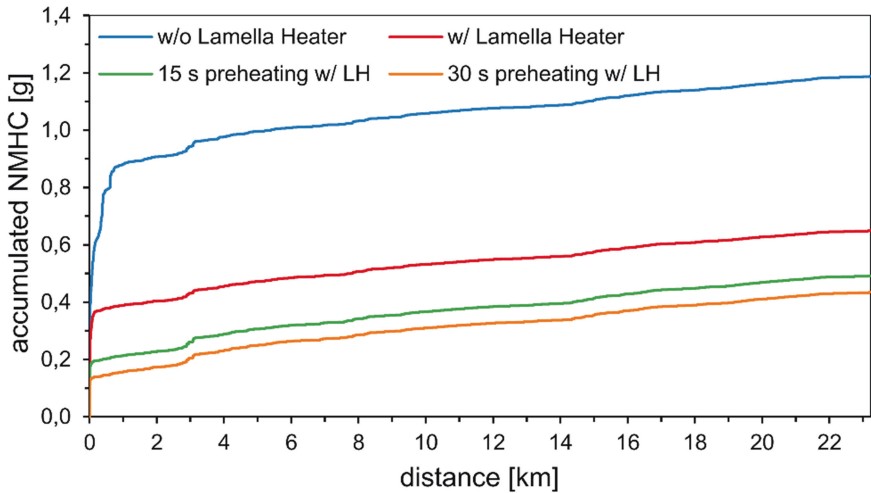


**Fig. 11.** Effects of heating strategy on NMHC emissions at a 1.5 L Otto-Engine.

The green line in Fig. 11 shows a preheating time of 15 s without air flow. This reduces emissions after the first kilometer by a further 45% compared to the case with heating starting from engine start. A further extended preheating period of 30 s without flow is shown by the orange line. This results in a further emission reduction after the first kilometer by another 23%.

A decisive factor for emission reduction in gasoline engines is the rapid heating of the catalyst during cold start within the first 60 s after engine start. Therefore, the influence of different heating strategies on the cumulative NMHC emissions over the first kilometer of the WLTC driving distance is shown in Fig. 12.

**Preheating with mass flow before engine start.** Electric preheating before engine start is also frequently considered in conjunction with a carrier air flow. To generate the carrier air flow before engine start, either a secondary air blower is required or air via an electric turbocharger has to be used. In addition to the additional energy expenditure, the additional components in the case of the secondary air blower must also be considered. Therefore, the aim should be to be able to perform preheating without carrier air flow, while maintaining the same efficiency. This possibility is also determined by the geometry and heat capacity of the heater. Studies on preheating with carrier air flow have been carried out for different mass flows and preheating durations. In the following, preheating with a carrier air flow of 45 kg/h is compared to preheating without air flow. Figure 12 shows the effect on NMHC emissions in the WLTC. Again, the blue line shows the unheated case. The red line shows the start of heating at engine start. The green line shows a preheating period of 15 s without air flow. The purple line shows a preheating duration of 15 s with a carrier air flow of 45 kg/h. The comparison shows lower emissions for preheating without carrier air flow.